Yurpolskaya L. A.[1], Shlyappo M. A.[1], Makarenko V. N.[1],
Svobodov A. A.[1], Levchenko E. G.[1], Makarenko M. V.[1], Poromov A. A.[2]

[1] A.N. Bakoulev Scientific Center for Cardiovascular Surgery, Moscow, Russia

[2] I. Mechnikov Research Institute of Vaccines and Sera, Moscow, Russia

4D FLOW Magnetic Resonance Imaging in the Study of Blood Flow in Patients With Aortic Coarctation in the Long-Term After Surgery

Aim	Comprehensive evaluation of blood flow in the thoracic aorta using a software for 4D processing of magnetic resonance (MR) images of the heart and blood vessels (4D Flow) in patients with aortic coarctation in the late postoperative period.
Materials and methods	The MR study of the heart was performed for 10 patients (7 boys and 3 girls) aged 8 to 13 years (median, 9.5 [8.3; 10.8] years) who underwent resection with end-to-end anastomosis for aortic coarctation at age of 2 weeks to 10 months. MR tomography was performed on a 1.5 T MR scanner using a multichannel surface coil for scanning, electrocardiographic synchronization, and a specialized package of pulse sequences for scanning of the heart. Blood flow was evaluated with a 4D data handling software for processing of MR images of heart and blood vessels (4D Flow). The following blood flow parameters were analyzed: blood flow volume per second, peak blood flow velocity, peak and minimum blood flow area at the levels of ascending aorta, arch, isthmus, and descending aorta, and pressure gradient at the level of maximum narrowing of the aorta. 3D–MR images were used for evaluation of aortic geometry. Blood flow formation, distribution, and trajectories were analyzed by maps of vectors, particle trace, and stream lines. Statistical analysis was performed with a Statistica (v. 6.0 StatSoft Inc.) package.
Results	Accelerated flow in the region of residual aortic stenosis in systole was observed in all patients; 4 patients had an additional vortex flow below the aortic stenosis and a spiral flow in the descending aorta. The pressure gradient on the aortic isthmus was directly correlated with the left ventricular myocardial mass index (r=0.65; p=0.04) and indexes of blood flow in the ascending and descending aorta (p=0.03; p=0.026). No significant correlation was found for blood flow indexes and geometry of the aortic arch (H/L). Delayed contrast enhancement MR imaging did not detect any fibrotic changes in the myocardium in only one patient. The fibrosis severity inversely correlated with the right ventricular ejection fraction (r=0.65; p=0.04) and directly correlated with the pressure gradient at the aortic isthmus (r=0.63; p=0.05).
Conclusion	The 4D MR image processing software for the heart and blood vessels allows studying the blood flow in detail under natural conditions, provides potential advantages in comprehensive evaluation of patients with aortic coarctation during a dynamic follow-up. For a definitive conclusion about the relationship between the altered blood flow in the thoracic aorta and markers of residual, post-correction pathology, larger studies are required as well as long-term follow-up of patients with documented pathological patterns of blood flow (changes in blood flow velocity and volume throughout the entire thoracic aorta in combination with disorders in the normal flow geometry during the cardiac cycle).

Keywords 4D flow magnetic resonance imaging; aortic coarctation; heart defects

For citation Yurpolskaya L.A., Shlyappo M.A., Makarenko V.N., Svobodov A.A., Levchenko E.G., Makarenko M.V. et al. 4D FLOW Magnetic Resonance Imaging in the Study of Blood Flow in Patients With Aortic Coarctation in the Long-Term After Surgery. Kardiologiia. 2020;60(8):54–64. [Russian: Юрпольская Л. А., Шляппо М. А., Макаренко В. Н., Свободов А. А., Левченко Е. Г., Макаренко М. В. и др. Методика 4D магнитно-резонансной томографии потока в изучении кровотока у пациентов с коарктацией аорты в отдаленные сроки после операции. Кардиология. 2020;60(8):54–64]

Corresponding author Yurpolskaya L. A. E-mail: layurpolskaya@bakulev.ru

Coarctation of the aorta (CoAo) is very well known and has been described in past centuries. Nevertheless, it is still of interest to modern researchers and physicians. According to the world's leading heart surgery clinics, children with surgically repaired CoAo at neonatal and early age are still at a high risk of severe complications (hypertension, heart rhythm disorders, cerebrovascular diseases, aortic and cerebral aneurysm, acute coronary syndrome) and sudden death at a young age [1–4]. It has been proven that surgical repair of CoAo does not restore normal aortic hemodynamics, although significantly reducing the pressure gradient across the aortic isthmus. Furthermore, hemodynamic changes in these patients are not localized in the aortic isthmus and are extended over

ISSN 0022-9040. Kardiologiia. 2020;60(8). DOI: 10.18087/cardio.2020.8.n1094

the entire vessel [1–5]. Since such patients are at a high risk of disability at a young age, it is important to develop and perform a multi-system examination of children to detect predictors of the complications and eliminate them as much as possible. Therefore, long-term post-surgery case follow-up with a detailed study of structural hemodynamic features is particularly essential for a deeper understanding of the process pathophysiology [2, 4, 5].

Magnetic resonance imaging (MRI) of the heart and its breakthrough technologies of scanning and image processing seems to be most attractive for case follow-up. One of such new magnetic resonance (MR) techniques is the 4D Flow image processing for the blood flow assessment. Its clinical use expectedly generates a growing interest worldwide [6–10].

The technique allows a retrospective visualization of blood flow 3D geometry, velocity color mapping, blood flow direction in random parts of the vascular system, and blood flow measurement. Free-breathing scanning is performed without contrast enhancement and can be used at various stages of case follow-up, making this technique particularly attractive for pediatric patients [2, 5, 6, 8].

We have been using this technique for the diagnosis of various cardiovascular diseases since 2012. The results have proved to be clinically relevant, prompting us to begin studying the physiological features of circulation in patients with CoAo. Our first findings are presented in this paper.

The aim of the study was to perform a comprehensive assessment of thoracic aorta blood flow using 4D Flow MRI in patients with CoAo in the long-term post-operative period.

Material and Methods

An MRI examination was performed in 10 patients (7 male and 3 female) aged 8 to 13 (median age 9.5 [8.3; 10.8] years old) who had undergone an extended resection and end-to-end anastomosis for CoAo at the age of between 2 weeks and 10 months. The post-operative pressure gradient was 28.5 [22.8; 32] mm Hg at discharge. It should be noted that two patients were subjected to balloon angioplasty twice before the resection of CoAo, while one 6-year-old patient underwent a resection of a false aneurysm in the anastomosis area.

At the time of the MRI examination, all patients had already been followed up. No ethical approval was thus required. The patient survey revealed fatigue and leg pains during physical activity, periodic headaches.

Parents signed informed consent for MRI before the examination. MRI examination was performed on an Avanto 1.5 T scanner, using a multi-channel surface scanning coil, electrocardiographic gating, and special cardiac scanning package.

The standard cardiac scan protocol included pulse sequences: fast-spin echo (TRUFI: time of echo (TE)= 1.2–1.4 ms, α=70–80°) to assess cardiac anatomy, time of repetition (TR) =RR interval and heart rate (HR) dependent, number of slices=10–15; transverse and oblique slices of the regions of interest. The breath-hold cine-MRI was performed to evaluate the functional parameters of the heart (TRUFISP: TE=1.1–1.2 ms; HR-dependent TR, α=60–70°), 20–30 phases; the 4-, 2-chamber views of the left ventricle (LV) and in the short-axis view were used. The slice thickness was 4–8 mm for both sequences.

Late gadolinium enhancement (LGE) of the myocardium was used after 3D MR angiography with intravenous contrast enhancement, in order to identify possible fibrotic changes in the myocardium. Gadolinium-containing agent 0.15–0.2 mmol/kg was injected with an automatic injector at the rate of 3–4 ml/s. The result was evaluated 15 minutes after the injection using Phase Sensitive Inversion Recovery (PSIR) turbo FLASH sequence, TE=1,2 ms, α=45°. The Time of Inversion (TI) was selected based on the MR signal intensity in the myocardium equal to 0, followed by the late enhancement altered over time (TI=200 to 320 ms).

Conventional 2D phase contrast-enhanced MRI (PC MRI) of the aortic parts of interest in the transverse view and 3D-coded scanning for subsequent 4D image processing was used to assess blood flow. Velocity encoding was selected individually in all protocols, starting from standard VENC=150 cm/s. The examination was free-breathing with the use of relevant compensation protocols. The 4D Flow 3D PC scan protocol included Voxel 2.2×1.7×5.0 mm, TR=79.1 ms, TE=3.39 ms, FOV=320×75, α=15°, matrix=108×192, time of scanning 10–15 min, 5 mm slices; VENC=150 cm/s; the encoding velocity was increased in case of artifacts during the selection; time resolution was 40–50 ms. The thoracic aorta was scanned from the LV exit pathway up to the diaphragm.

The results were evaluated using tailored cardiac image processing software packages Argus and Q-mass and the 4D Flow package, version 4, for blood flow assessment. The analysis included calculating volumes and ejection fractions (EF) of both ventricles, linear dimensions of cardiac chambers and vessels, number of foci of contrast uptake in the LV and right ventricle (RV) their localization, spread, and intensity.

The following blood flow measures were analyzed: blood flow volume per second; peak flow rate, maximum and minimum flow area (Smaxfl and Sminfl) at the levels of interest. These levels were: ascending aorta (AAo), aortic arch (AoA), aortic isthmus (AoI), descending aorta (DAo); cardiac cycle synchronization graphs (measure-time cur-

ve); and the pressure gradient at the level of maximum aortic narrowing. The aortic geometry was analyzed in 3D MR images based on the height (H) and width (L) of the arch and their ratio calculated according to Ou et al. [11]. The formation, distribution and paths of blood flow were analyzed by vector maps, particle trace, and stream line.

Additional standard brain MRI examinations and time-of-flight (TOF) non-contrast-enhanced MR angiography with the scanning of extra-intracranial zones were carried out to identify possible changes in the brain and brachiocephalic vessels.

A statistical analysis of data was carried out in the Statistica 6.0 software suite (StatSoft Inc). The significance of the differences was determined using the non-parametric Mann-Whitney U-test. The data is presented as the median and interquartile range Me [Q1; Q3]. The correlations between the values were estimated using the correlation analysis with the Spearman correlation coefficient (r). The differences were significant at $p<0.05$.

Results

The main MRI data is shown in Table 1.

The blood flow area, volume, and velocity at the levels of interest are provided in Table 2.

4D image processing data analysis identified the significant differences only of the isthmus and descending aorta blood flow volume from that in the ascending aorta and aortic arch. Differences in the peak flow velocities in the regions of interest were not significant. The isthmus pressure gradient obtained with the 4D processing was 8.0 [6.5; 9.6] mm Hg and not significantly different from 2D PC MRI with 10.6 [3.3; 16] mm Hg.

The velocity measurement was clearly displayed on the 4D Flow color map. The particle trace and stream line protocols allowed us to visualize the directions of the flow and its components during the different phases of the cardiac cycle. The normal aortic flow lines have smooth paths on the 4D Flow maps without abnormal secondary flow components (Figure 1).

Analysis of the 4D blood flow maps revealed that all patients showed an acceleration of flow and even a loss of signal during the systole in the area of minimal residual narrowing of the aorta, both local and extended (Figure 2).

Furthermore, four patients had an additional vortex below the mild narrowing of the aorta and a helix in the descending aorta, which persisted throughout the diastole (Figure 3).

The same patients also had increased blood flow at the level of anastomosis throughout the diastole. They also had accelerated blood flow toward the brachiocephalic vessels and evident changes in the brain MR images. The map analysis identifies increased velocity in the arch in five children. Four of them had aneurysmatic dilation of the ascending aorta.

Brain MRI and brachiocephalic angiography showed an asymmetry of the internal carotid arteries (ICAs) in five patients, hypoplasia of a vertebral artery (VA) in three children, an asymmetric ICA combined with the blood flow asymmetry in the VA in one child, and a tortuosity of the VCA in one more child. Vascular changes were combined with brain pathologies in five patients. For example, one patient had a focal lesion in the white matter of the brain, another one had dilated perivascular spaces, while two more patients had retrocerebelular cysts, and one child had a periventricular cyst. The correlation analysis revealed a significant inverse relationship between the brain pathologies and RVEF ($r=0.63$; $p=0.05$).

In only one patient the delayed MR contrast evaluation detected no fibrotic changes in the myocardium. The lesion was assessed depending on the extension and number of myocardial segments involved. Of the ten patients studied, seven had RV free wall lesion as well as LV fibrotic changes (Figure 4).

Table 1. MRI profile of the patients examined

Parameter	Value
LV end-diastolic volume, mL	63.5 [59.8; 73]
LV end-diastolic volume index, mL/m^2	61.1 [54.4; 74.6]
LV end-systolic volume, mL	17 [13.5; 19.9]
LV end-systolic volume index, mL/m^2	16.1 [13.5; 19.1]
LV systolic volume, mL	49.5 [43.3; 56.5]
LV systolic volume index, mL/m^2	42.9 [39.3; 56.3]
LV ejection fraction, %	75 [68.8; 79.3]
Minute volume, mL/min.	4.54 [3.7; 5.3]
Cardiac index, L/min/m2	4.2 [3.7; 4.7]
LV mass, g	49.8 [47.0; 53.3]
LV myocardial mass index, kg/m^2	46.1 [42.8; 52.9]
RV ejection fraction, %	63.5 [62; 64.8]
Ascending aorta diameter, mm	18 [18; 22]
Aortic arch diameter, mm	10 [9; 11.5]
Aortic isthmus diameter, mm	8 [7.3; 9]
Post-isthmus diameter of the aorta, mm	11.5 [10.3; 13]
Descending aorta diameter, mm	11 [10; 12]
Arch height H, mm	29.5 [25.3; 30.8]
Arch width L, mm	43.5 [41.3; 46.5]
H/L ratio	0.65 [0.6; 0.7]

The data is presented as the median and interquartile range Me [Q1; Q3]. MRI, magnetic resonance imaging; LV, left ventricle; RV, right ventricle.

ISSN 0022-9040. Kardiologiia. 2020;60(8). DOI: 10.18087/cardio.2020.8.n1094

Table 2. Area, volume, and blood flow velocity according to 4D Flow MR image processing at different levels

Parameter	AAo	AoA	AoI	DAo
Blood flow volume, mL/s	41.5 [37; 43.5]	36.5 [35; 39.5]	26 [19.8; 34.5]	21.5 [17; 30.5]
Max. blood flow velocity, cm/s	122.5 [112; 155.8]	120.5 [106; 139.8]	162.5 [91.3; 201.3]	102.5 [95.5; 118.3]
Max. flow area, mm^2	362 [289.6; 432.1]	96.5 [74.9; 102.1]	72.8 [57.1; 89.4]	143.6 [110.2; 213.1]
Min. flow area, mm^2	313.2 [242.9; 432.1]	80.8 [65.2; 87.6]	58.9 [58.8; 76.0]	97.8 [81.0; 144]
Changes in blood flow area S from max., %	13.5 [16.4; 11.1]	13.05 [16.8; 12.1]	14.5 [16.2; 14.2]	32 [33.8; 29.0]

The data is presented as the median and interquartile range Me [Q1; Q3].
AAo, ascending aorta; AoA, aortic arch; AoI, aortic isthmus; DAo, aorta descending.

The severity of fibrosis was inversely correlated with RVEF (r=0.65; p=0.04) and directly correlated with the aortic isthmus pressure gradient (r=0.63; p=0.05). The results of the correlation analysis of aortic dimensions and pressure gradients at the different measurement levels are provided in Table 3.

The peak velocity and systolic volume of the blood flow are not significantly correlated with the arch geometry (height H, width L, and H/L ratio). The arch geometry was associated with several anthropometric and LV measurements (see Table 3). The peak velocities and volumes of the blood flow in the aorta were expectedly directly correlated. There was also a correlation between blood flow values and LV volumes. The correlations between the peak velocity and systolic volume of the aortic blood flow were slightly different at the different levels of interest (Table 4).

Figure 1. 4D Flow Color Mapping and Stream Line MRI findings in the thoracic aorta in a healthy 12-year-old child

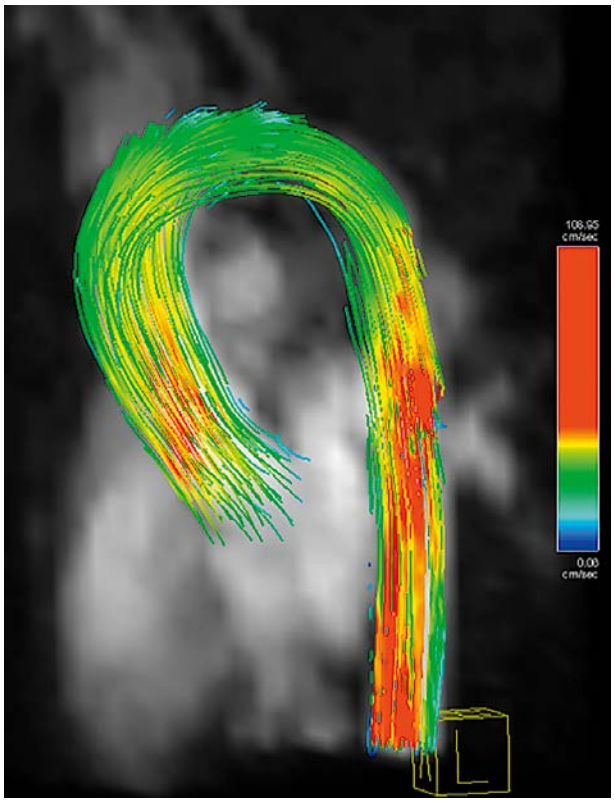

Here and in Figures 2, 3: the color corresponds to certain velocity values with the highest velocity indicated in red. MRI, magnetic resonance imaging.

Figure 2. 4D Flow Color Mapping and Stream Line MRI findings in the thoracic aorta in children with resected aortic coarctation

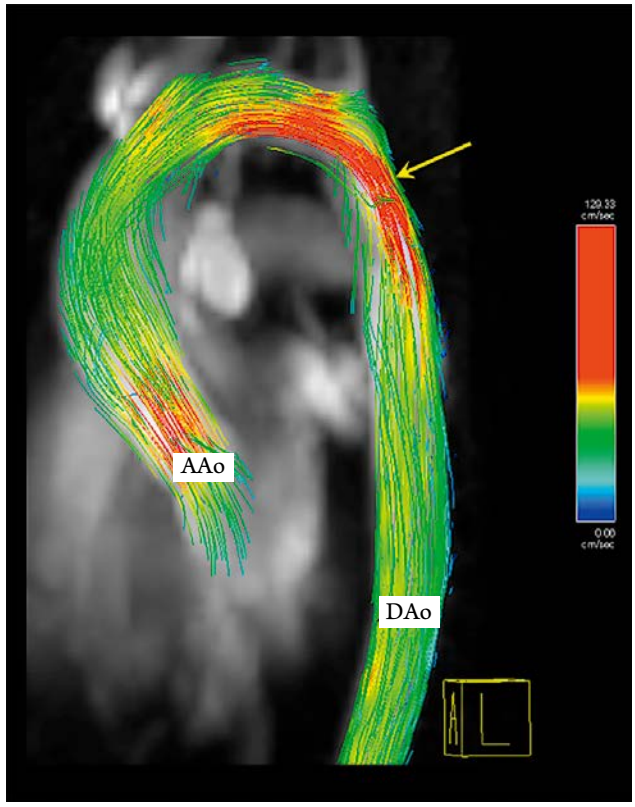

Increased flow velocity in the arch and isthmus (arrow), no increase in the blood flow velocity in the distal descending thoracic aorta. AAo, ascending aorta; DAo, descending aorta.

It is generally possible to state that the blood flow in the aorta at the different levels is differentiated by the age-related anatomic features of patients and the heart's functional measurements, it was also associated with both the left heart measurements and with RVEF. These findings are to be confirmed in a larger statistical sample.

Discussion

The primary benefit of 4D MR imaging of the heart and vessels is its ability to show blood flow at the level of interest as a 3D model throughout the cardiac cycle. Using this protocol in patients with CoAo a single MRI examination allows for the calculation of collateral blood flow. It also evaluates the thoracic aortic flow velocity profiles, and complex secondary blood flow characteristics that are poorly visualized by other methods [2].

The state-of-the-art fundamental sciences have enabled us to reveal characteristic patterns of the blood flow (flow geometry and contours in different phases of the heart cycle) in a healthy thoracic aorta: helix flow along the right helix and moderate early diastolic retrograde flow in the ascending aorta [12]. The flow velocities are maximum in the ascending aorta, and lower in the arch when the flow propagates to the brachiocephalic branches. They increase in the proximal descending aorta at the point where the flow paths separate from the inner curvature and merge into one at the outer wall. The early-diastole retrograde flow goes along the internal pathways of the ascending aorta and the proximal descending arch, contributing to the diastolic filling of the coronary arteries [12].

The age and diameter of the ascending aorta were the most accurate predictors of the vortex. The helix was found to be typical of standard arcuate aortic forms and decrease with age. This data emphasizes the relevance of age and geometry in the hemodynamic assessment in different age groups [13].

In our study, the blood flow velocity, on the contrary, increased in the arch and decreased in the descending aorta despite a physiological narrowing. Furthermore, the 4D processing of the descending aorta images showed a pronounced helix and vortex flow in the post-stenotic dilation areas in all patients. The presence of a «gothic» aortic arch may serve as an explanation for this abnormal helix flow in the descending thoracic aorta. However, we did not find direct correlations. Given the relationship between arch geometry and hypertension described in the literature, the presence of an apparent abnormal helix blood flow in the descending aorta may be associated with the development of systemic arterial hypertension [2, 10, 14, 15].

We did not receive such explicit data confirming the dependence of the blood flow parameters on a shape of the arch, which is described in the literature [11, 14]. The arch geometry did not determine the velocity and pressure gradient but was more correlated with the age-related anatomic parameters and myocardial volume and mass indices. This data is consistent with the findings of Quail et al. [16], who studied the major changes in the 3D aortic

Figure 3. 4D Flow Color Mapping and Particle Trace MRI findings in the thoracic aorta after the resection of aortic coarctation

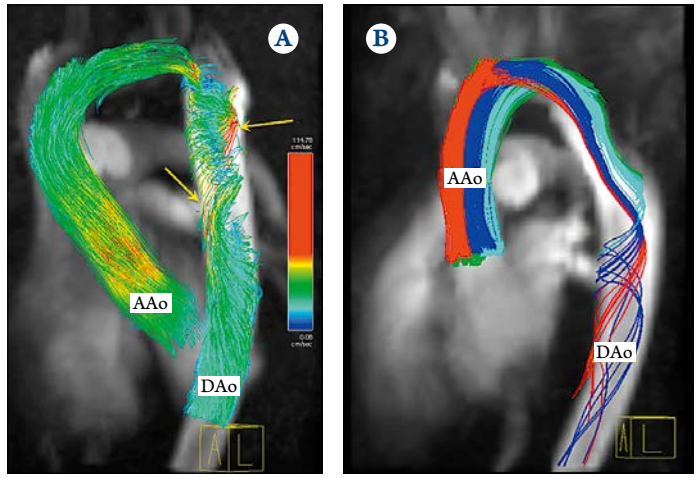

A – additional vortex and propagation of a helix in the descending aorta (arrows); B – zoning of the flow particles involved in the formation and propagation of the helix in the descending thoracic aorta; AAo, ascending aorta; DAo, descending aorta.

Figure 4. Delayed Contrast Enhancement MR imaging of the heart: short-axis view at the mid-third level of the left ventricle, contrast agent accumulation in the fibrous myocardium (high MR signal)

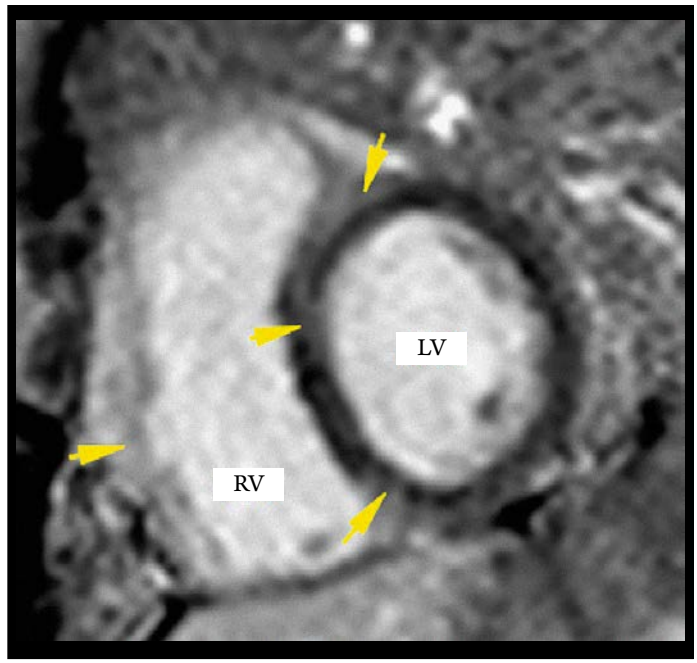

LV, left ventricle; RV, right ventricle.

ISSN 0022-9040. Kardiologiia. 2020;60(8). DOI: 10.18087/cardio.2020.8.n1094

ДЕЛАЙ ПРОЩЕ
ДЕЛАЙ ЛУЧШЕ

Импликор®

1 таблетка 2 раза в сутки

Ивабрадин + Метопролол

Больше возможностей в одной таблетке для пациентов со стабильной стенокардией!

В 6 раз меньше приступов стенокардии[1]	Лучше переносимость физической нагрузки[1]	Выше качество жизни пациента[1]	Отличная переносимость лечения[1]

ИНСТРУКЦИЯ ПО ПРИМЕНЕНИЮ ПРЕПАРАТА ИМПЛИКОР®.

СОСТАВ*. Импликор® 5мг/25мг: 5 мг ивабрадина/25 мг метопролола; Импликор® 7,5мг/25мг: 7,5 мг ивабрадина/25 мг метопролола; Импликор® 5мг/50мг: 5 мг ивабрадина/50 мг метопролола; Импликор® 7,5 мг/50 мг: 7,5 мг ивабрадина/50 мг метопролола. Показания к применению*. Симптоматическое лечение стабильной стенокардии у взрослых пациентов с нормальным синусовым ритмом, состояние которых адекватно контролировалось применением комбинации монопрепаратов ивабрадина и метопролола в тех же дозах. СПОСОБ ПРИМЕНЕНИЯ И ДОЗЫ*. 1 таблетка 2 раза в сутки, утром и вечером, во время еды, запивая достаточном количеством жидкости. Концентрация метопролола в плазме крови повышается при одновременном приёме с пищей. Этот факт должен учитываться при лечении пациентов, которые принимали метопролол натощак перед назначением препарата Импликор®. При необходимости коррекцию дозы следует проводить монопрепаратами ивабрадина и метопролола. При почечной недостаточности: при величине клиренса креатинина выше 15 мл/мин не требуется изменения дозы. При снижении клиренса креатинина ниже 15 мл/мин применять с осторожностью. При печеночной недостаточности: у пациентов с печеночной недостаточностью средней степени тяжести применять с осторожностью, пациентам с печеночной недостаточностью тяжелой степени тяжести препарат противопоказан. Пациенты пожилого возраста: с осторожностью. Применение у детей и подростков: противопоказан (эффективность и безопасность применения у данной возрастной группы не установлена). Противопоказания*. Повышенная чувствительность к ивабрадину, метопрололу (и другим препаратам группы бета-адреноблокаторов ввиду возможной перекрестной чувствительности), а также к вспомогательным веществам; выраженная или симптоматическая брадикардия; кардиогенный шок; острый инфаркт миокарда (ОИМ) или подозрение на ОИМ, осложненный выраженной брадикардией, атриовентрикулярной блокадой I степени, артериальной гипотензией (АГ) (систолическое артериальное давление (АД) менее 100 мм рт.ст.) и/или тяжелой сердечной недостаточностью; синдром слабости синусового узла (включая, синоатриальную блокаду); атриовентрикулярная блокада (AV) II и III степени; тяжелая артериальная гипотензия (АД менее 90/50 мм рт.ст.) или симптоматическая артериальная гипотензия; нестабильная или острая сердечная недостаточность; у пациентов, периодически получающих кратковременное лечение бета-адреномиметиками; пациенты, зависимые от кардиостимулятора (у которых сердечный ритм обеспечивается только постоянной кардиостимуляцией); нестабильная стенокардия; тяжелое заболевание периферических сосудов; нелеченая феохромоцитома; тяжелая печеночная недостаточность; метаболический ацидоз; одновременное применение с мощными ингибиторами изоферментов CYP3A4, такими как противогрибковые средства группы азолов (кетоконазол, итраконазол), антибиотики группы макролидов (кларитромицин, эритромицин для приема внутрь, джозамицин, телитромицин), ингибиторы ВИЧ протеазы (нелфинавир, ритонавир) и нефазодон; одновременное применение с верапамилом или дилтиаземом; беременность, грудное вскармливание и применение женщинами с сохраненным детородным потенциалом, не использующими надежные методы контрацепции; возраст до 18 лет (эффективность и безопасность применения в данной возрастной группе не изучалась). ОСОБЫЕ УКАЗАНИЯ*. Пациенты с умеренно выраженной печеночной недостаточностью (менее 9 баллов по шкале Чайлд-Пью): с осторожностью. Недостаточность положительного эффекта в отношении клинических исходов у пациентов с симптоматической стабильной стенокардией: в качестве симптоматической терапии стабильной стенокардии, поскольку ивабрадин не оказывает положительного эффекта на частоту сердечно-сосудистых событий (например, инфаркт миокарда или смерть вследствие сердечно-сосудистых причин) у таких пациентов. Контроль ЧСС: определение ЧСС в покое у пациентов, принимающих ивабрадин, при принятии решения о коррекции дозы должно быть выполнено одним из указанных способов: серийное измерение ЧСС, ЭКГ или 24-часовое амбулаторное мониторирование ЭКГ. Нарушения сердечного ритма: Импликор® не рекомендуется пациентам с фибрилляцией предсердий или другими типами аритмий, связанными с функцией синусового узла. Повышен риск развития фибрилляции предсердий. Необходимо регулярное клиническое наблюдение за пациентами для своевременного выявления фибрилляции предсердий. Если в период лечения возникла фибрилляция предсердий, соотношение ожидаемой пользы к возможному риску при дальнейшем применении ивабрадина должно быть еще раз тщательным образом проанализировано. Пациенты с хронической сердечной недостаточностью (ХСН) и нарушениями внутрижелудочковой проводимости (блокада левой или правой ножки пучка Гиса) и желудочковой диссинхронией должны находиться под пристальным контролем. Применение у пациентов с низкой ЧСС: противопоказан, если до начала терапии ЧСС в покое составляет менее 70 уд. Если на фоне терапии наблюдается стойкое снижение ЧСС в покое менее 50 уд/мин, или у пациента возникают симптомы, связанные с брадикардией, необходимо уменьшить дозу препарата, перейдя на прием препаратов на основе монокомпонентов, до достижения оптимальной дозы метопролола, или отменить лечение. Комбинированное применение с блокаторами «медленных» кальциевых каналов (БМКК): противопоказано. ХСН: у пациентов с ХСН IV ФК по классификации NYHA применять с осторожностью. Инсульт: не рекомендуется назначать препарат сразу после перенесенного инсульта. AV I степени: с осторожностью. Тяжелые нарушения функции почек (клиренс креатинина менее 15 мл/мин): с осторожностью. Функции зрительного восприятия: применять с осторожностью у пациентов с пигментной дегенерацией сетчатки. Отмена терапии: нельзя резко отменять бета-адреноблокаторы. Прекращение приема должно сопровождаться одновременным приемом метопролола в виде монокомпонентного препарата в оптимальной для пациента дозе. Если необходимо, применение ивабрадина можно прекратить резко. Дозу метопролола следует снижать постепенно, желательно, в течение не менее 2 недель, одновременно начиная заместительную терапию, если необходимо. В случае появления у пациента любых симптомов отмены, снижение дозы должно быть более постепенным. Артериальная гипотензия: с осторожностью, при тяжелой артериальной гипотензии (АД менее 90/50 мм рт.ст.) применение противопоказано. Фибрилляция предсердий – сердечные аритмии: плановую электрическую кардиоверсию следует проводить не ранее, чем через 24 часа после приема последней дозы ивабрадина. Применение у пациентов с врожденным синдромом удлиненного интервала QT или у пациентов, принимающих препараты, удлиняющие интервал QT: не следует назначать. Применение у пациентов с артериальной гипертензией, которым требуется изменение антигипертензивной терапии: терапия должна сопровождаться регулярным контролем АД. Применение у пациентов с бронхиальной астмой и ХОБЛ: с осторожностью и при необходимости назначать бронходилатирующие средства. Тяжелые поражения периферических сосудов: следует отменить препарат и подобрать индивидуальные дозы монокомпонентных препаратов. Феохромоцитома: при подтвержденном или предполагаемом диагнозе феохромоцитомы применять бета-адреноблокаторы следует в комбинации с альфа-адреноблокаторами. Пациенты с сахарным диабетом: следует применять с осторожностью (бета-адреноблокаторы могут маскировать некоторые симптомы гипогликемии, в том числе, тахикардию). Стенокардия Принцметала: применение бета-адреноблокаторов может увеличить продолжительность и частоту приступов стенокардии Принцметала. Применение кардиоселективных бета1-адреноблокаторов возможно в случае минимальных и ассоциированных форм заболевания и только в сочетании с вазодилататорами. Псориаз: можно применять только после тщательной оценки соотношения пользы и риска. Тиреотоксикоз: симптомы тиреотоксикоза могут маскироваться при приеме бета-адреноблокаторов. Общая анестезия: необходимо предупредить врача-анестезиолога о проводимом лечении. Если необходима отмена бета-блокатора, применение препарата прекращают постепенно. Полностью прием препарата должен быть прекращен за 48 часов до общей анестезии. Пациенты пожилого возраста: необходимо тщательно контролировать клиническое состояние пожилых пациентов, поскольку чрезмерное снижение АД или ЧСС может привести к недостаточному кровоснабжению жизненно важных органов. Аллергические реакции: с осторожностью, так как метопролол может повышать чувствительность к аллергенам и усиливать тяжесть анафилактических реакций. У спортсменов: следует принимать во внимание возможность получения положительных результатов допинг-теста. ВЗАИМОДЕЙСТВИЕ С ДРУГИМИ ЛЕКАРСТВЕННЫМИ СРЕДСТВАМИ*. Противопоказанные сочетания: мощные ингибиторы изофермента CYP3A4; умеренные ингибиторы изофермента CYP3A4 (дилтиазем или верапамил), бета-адреномиметики. Нежелательные сочетания: лекарственные средства, удлиняющие интервал QT, грейпфрутовый сок, барбитураты, гипотензивные лекарственные препараты центрального действия, антиаритмические препараты I класса. Сопутствующее применение с осторожностью: калийнесберегающие диуретики (тиазидные и «петлевые» диуретики), другие умеренные ингибиторы изофермента CYP3A4, индукторы изофермента CYP3A4, индукторы изофермента CYP2D6, ингибиторы изофермента CYP2D6, лидокаин, ингаляционные анестетики, нитраты, сердечные гликозиды, бета-адреноблокаторы и ингибиторы моноаминооксидазы, адреналин, парасимпатомиметики, нестероидные противовоспалительные препараты, инсулин и пероральные сахароснижающие препараты. Комбинации, которые нужно принимать во внимание: трициклические антидепрессанты, нейролептики, мефлохин, дипиридамол (в/в), альфа-адреноблокаторы, применяемые в урологии, эрготамин, курареподобные миорелаксанты, флоктафенин, антациды. БЕРЕМЕННОСТЬ И ПЕРИОД ЛАКТАЦИИ*. Противопоказан. Влияние на способность управлять транспортными средствами и выполнять работы, требующие высокой скорости психомоторных реакций*. Пациентов следует предупредить о возможных нежелательных симптомах (таких как головная боль, головокружение, повышенная утомляемость), которые могут усиливаться на фоне приема алкоголя или изменении терапии. ПОБОЧНОЕ ДЕЙСТВИЕ*. Очень часто: изменения световосприятия (фосфены), повышенная утомляемость. Часто: ночные кошмары, патологические сновидения, головная боль, бессонница, сонливость, головокружение, нечеткость зрения, брадикардия, AV блокада I степени (удлинение интервала PQ на ЭКГ); желудочковая экстрасистолия, ощущение сердцебиения, неконтролируемое АД, фибрилляция предсердий, ощущение похолодания конечностей, болезнь Рейно, ортостатическая гипотензия, одышка при физической нагрузке, тошнота, запор, диарея, боли в животе, рвота, нарушение либидо. Нечасто: эозинофилия, обострение псориаза, гиперурикемия, гипогликемия, депрессия, спутанность сознания, галлюцинации, замедление скорости психических и двигательных реакций, понимания, эпизоды потери сознания, парестезии, ступор, нарушение зрения, синдром «сухого» глаза, раздражение конъюнктивы, диплопия, вертиго, атриовентрикулярная блокада I степени, ощущение сердцебиения, суправентрикулярные экстрасистолы, сердечная недостаточность, кардиогенный шок, боль в грудной клетке, артериальная гипотензия, перемежающаяся хромота, снижение АД, одышка, бронхоспазм, ангионевротический отек, кожная сыпь, дистрофические изменения кожи, крапивница, гипергидроз, псориаз, мышечные судороги, мышечные спазмы, астения, отеки, увеличение массы тела, повышение концентрации кратинина в плазме крови, удлинение интервала QT на ЭКГ. Редко: тромбоцитопения, повышенная возбудимость, тревога, снижение продукции слезы, конъюнктивит, шум в ушах, нарушения ритма сердца, нарушение проводимости миокарда, ринит, сухость слизистой оболочки полости рта, дисгевзия, отклонения показателей функции печени, нарушения функции печени, эритема, кожный зуд, алопеция, мышечная слабость, недомогание, повышение активности «печеночных» трансаминаз, половая дисфункция/импотенция. Очень редко: лейкопения, деперсонализация, амнезия, ксерофтальмия, нарушение слуха, снижение слуха, глухота, AV блокада II и III степени, синдром слабости синусового узла, учащение и утяжеление приступов у пациентов со стенокардией, сухая гангрена, ретроперитонеальный фиброз, гепатит, реакции фотосенсибилизации, артралгия, болезнь Пейрони. ПЕРЕДОЗИРОВКА*. ФАРМАКОЛОГИЧЕСКОЕ ДЕЙСТВИЕ*. Ивабрадин – препарат, замедляющий ритм сердца, механизм действия которого заключается в селективном и специфическом ингибировании If каналов синусового узла, контролирующих спонтанную диастолическую деполяризацию в синусовом узле и регулирующих ЧСС. Ивабрадин дозозависимо снижает ЧСС. Метопролол - кардиоселективный блокатор, блокирующий β_1-адренорецепторы (расположенные преимущественно в сердце) в дозах значительно меньших, чем дозы, требующиеся для блокирования β_2-адренорецепторов (локализованные, главным образом, в периферических сосудах и бронхах). Метопролол не обладает мембраностабилизирующей и внутренней симпатомиметической активностью.

ФОРМА ВЫПУСКА*: Таблетки, покрытые пленочной оболочкой, 5 мг + 25 мг, 7,5 мг + 25 мг, 5 мг + 50 мг, 7,5 мг + 50 мг. По 14 таблеток в блистер (ПВХ/Ал). По 1, 2, 4 и 6 блистеров с инструкцией по медицинскому применению в пачку картонную.

*Для получения полной информации, пожалуйста, обратитесь к инструкции по медицинскому применению лекарственного препарата.

1. Divchev D. et al. Cardiol Ther. 2017;6: 239-249. Дивчев Д. и соавт. Кардиология и терапия. 2017; 6: 239-249

Table 3. Correlation analysis of linear dimensions of the aorta and the pressure gradients

Data	d AAo	d AoA	d AoI	H	H/L	DAo grad	AoI grad
Age	ns	ns	r=-0.754 p=0.012	ns	ns	r=-0.633 p=0.049	ns
Height	ns	ns	ns	r=0.7859 p=0.007	ns	ns	ns
BMI	r=0.8753 p=0.001	ns	ns	ns	ns	ns	ns
BSA	ns	ns	ns	r=0.6479 p=0.043	ns	ns	ns
Duration of present history	ns	ns	r=-0.754 p=0.012	ns	ns	r=-0.633 p=0.049	ns
LVEDVI	ns	ns	ns	r=-0.6703 p=0.034	r=-0.739 p=0.015	ns	ns
LVESVI	ns	r=-0.5798 p=0.079	ns	ns	ns	ns	ns
LVSVI	ns	ns	ns	ns	r=-0.6898 p=0.027	ns	ns
CI	ns	ns	r=0.9163 p=0.000	ns	ns	r=0.7024 p=0.024	ns
LVEF	ns	ns	r=0.6209 p=0.055	ns	ns	ns	ns
MV	r=0.7668 p=0.010	ns	r=0.8048 p=0.005	ns	ns	ns	ns
LVMI	ns	ns	ns	r=-0.6882 p=0.028	r=-0.7358 p=0.015	ns	r=0.6516 p=0.041
RVEF	ns	ns	ns	ns	ns	ns	ns
AAo PV	r=0.8096 p=0.005	ns	r=0.7947 p=0.006	ns	ns	r=0.6436 p=0.045	ns
AoI PV	ns	ns	ns	ns	ns	ns	r=0.9871 p=0.000
DAo PV	ns	ns	ns	ns	ns	r=0.6353 p=0.048	r=0.6744 p=0.032
AAo PV %	ns	ns	ns	ns	ns	ns	r=0.6718 p=0.033
DAo SV	ns	ns	ns	ns	ns	r=0.5878 p=0.074	r=0.693-2 p=0.026
AAo SV %	ns	ns	ns	ns	ns	r=0.5723 p=0.084	r=0.6935 p=0.026
d DAo	ns	ns	ns	r=0.6314 p=0.050	ns	ns	ns
S % AAo flow	ns	ns	ns	ns	ns	r=0.7490 p=0.013	r=0.5712 p=0.085
S % DAo flow	ns	ns	ns	ns	ns	r=-0.7711 p=0.009	ns

ns, non-significant; grad, pressure gradient; AAo, ascending aorta; AoA, aortic arch; AoI, aortic isthmus; DAo, descending aorta, S, area; H, arch height; L, arch width; BMI, body mass index; LVEDVI, left ventricular end-diastolic volume index; LVESVI, left ventricular end-systolic volume index; LVSVI, left ventricular systolic volume index; CI, cardiac index; LVEF, left ventricular ejection fraction; MV, minute volume; LVMI, left ventricular mass index; RVEF, right ventricular ejection fraction; SV, systolic volume; PV, peak velocity; BSA, body surface area.

shape and blood flow values in patients with post-repair coarctation. They concluded that the shape is not the main determinant of vascular load after the recovery of the aortic isthmus lumen. Changes in vessel caliber are more important than the curvature.

It should be noted that secondary blood flow patterns (abnormal flow geometry and/or the presence of additional abnormal flows during the cardiac cycle), such as vortex blood flow, were detected at maximum systole not only in areas of moderate post-stenotic dilation but also

ISSN 0022-9040. Kardiologiia. 2020;60(8). DOI: 10.18087/cardio.2020.8.n1094

ISSN 0022-9040. Kardiologiia. 2020;60(8). DOI: 10.18087/cardio.2020.8.n1094

Table 4. Correlation analysis of blood flow measurements

Data	Age	Body weight	BMI	BSA	Duration of anoxia	LVEDV	LVESV	LVSV	LVEDVI	LVSVI	CI	LVEF	MV	LVM	LVMI	RVEF
AAo PV	ns	ns	r=0.6404 p=0.046	ns	ns	ns	ns	ns	ns	ns	r=0.6766 p=0.032	ns	r=0.7640 p=0.010	ns	ns	ns
AoA PV	ns	r=0.7699 p=0.009	r=0.7641 p=0.010	r=0.7046 p=0.023	ns	r=0.8014 p=0.005	ns	r=0.8252 p=0.003	ns	ns	ns	ns	r=0.9069 p=0.000	r=0.6453 p=0.044	ns	ns
AoI PV	ns	ns	ns	ns	ns	ns	ns	ns	ns	ns	ns	ns	ns	ns	r=0.6384 p=0.047	ns
DAo PV	ns	ns	ns	ns	ns	r=0.6658 p=0.036	ns	r=0.6459 p=0.044	r=0.6563 p=0.039	ns	ns	ns	ns	ns	ns	ns
AAo SV	ns	r=0.8105 p=0.004	r=0.7815 p=0.008	r=0.7381 p=0.015	ns	r=0.9166 p=0.000	r=0.6928 p=0.026	r=0.8783 p=0.001	ns	ns	ns	ns	r=0.8043 p=0.005	r=0.8049 p=0.005	ns	ns
AoA SV	ns	ns	ns	ns	ns	ns	ns	ns	ns	r=0.7190 p=0.019	ns	r=0.6656 p=0.036	ns	ns	r=0.6545 p=0.040	ns
DAo SV	ns	ns	ns	ns	ns	ns	ns	r=0.6341 p=0.049	r=0.7319 p=0.016	r=0.7705 p=0.009	r=0.6659 p=0.036	ns	ns	ns	ns	ns
Smax AAo flow	ns	ns	ns	ns	ns	ns	ns	ns	ns	ns	r=0.6803 p=0.030	ns	ns	ns	ns	r=0.7324 p=0.016
Smin DAo flow	r=-0.6313 p=0.050	ns	ns	ns	r=-0.6313 p=0.050	ns	ns	ns	ns	ns	ns	ns	r=0.6687 p=0.034	ns	ns	ns
S % AAo flow	r=-0.7947 p=0.006	ns	ns	ns	ns	ns	ns	ns	ns	ns	r=0.6143 p=0.059	ns	ns	ns	ns	ns
AoA flow S %	ns	ns	ns	ns	ns	ns	ns	ns	ns	ns	ns	ns	ns	ns	ns	r=0.6646 p=0.036
S % AoI flow	ns	ns	ns	ns	ns	ns	ns	ns	ns	ns	ns	ns	ns	ns	r=-0.6288 p=0.051	ns
S % DAo flow	r=0.8019 p=0.005	ns	ns	ns	r=0.8019 p=0.005	ns	ns	ns	ns	ns	r=-0.7667 p=0.010	ns	ns	ns	ns	ns

ns, non-significant; AAo, ascending aorta; AoA, aortic arch; AoI, aortic isthmus; DAo, descending aorta, S, area; Smin/max, minimum/maximum area; H, arch height; L, arch width; BMI, body mass index; LVEDVI, left ventricular end-diastolic volume index; LVESVI, left ventricular end-systolic volume index; LVSVI, left ventricular systolic volume index; CI, cardiac index; LVEF, left ventricular ejection fraction; MV, minute volume; LVMI, left ventricular mass index; RVEF, right ventricular ejection fraction; SV, systolic volume; PV, peak velocity; BSA, body surface area.

in the moderate anatomical narrowings of the descending aorta. Given the detected decrease rather than an increase in blood flow velocity and volume, changes in renal blood flow which cause increased renin-angiotensin-aldosterone (RAAS) activity may contribute to an increase in systemic blood pressure (BP). After surgery, the same mechanisms are most likely to be involved in preserving hypertension as those before the repair: increased activity of RAAS, modified vasoreactivity, abnormal geometry of the aortic arch, dysfunctional mechanism of baroreceptors, aortic wall rigidity [17, 18].

Our findings that the isthmus pressure gradient is correlated with LV hypertrophy and blood flow in the ascending and descending aorta, including changes in the flow area, may be indirectly indicative of the remodeling processes in both the LV and the aortic walls [5, 19]. The viscoelasticity of the aorta does not recover even after early neonatal surgical repair of coarctation. The decreased viscoelasticity of the ascending and descending aorta appears to be due to the systemic nature of vascular pathology [20, 21].

In our study, blood flow rates were more dependent in the aortic arch and descending aorta. For example, the arch pressure gradient was dependent on the patient's age and duration of the disease, as well as the LV functional parameters. This may partially explain more severe pathologies in patients with hypoplasia of the aortic arch. According to Ntsinjana et al. [22], residual hypoplasia of the aortic arch and narrowing of the isthmus were the main parameters affecting the pathophysiology of changes in BP during physical activities.

Thus, the common use of 4D Flow pressure maps showing changes in the spatial distribution of aortic pressure in coarctation seems to be promising in patients before and after surgery. This technique will help to identify pathophysiological conditions underlying the complications of the CoAo repair and determine the follow-up intervals and future management [10].

The direct correlation of the pressure gradient in the isthmus with the myocardial fibrosis and the LV mass index was expected in our study. Most of the children who had undergone surgery (7 of 10) experienced changes in the myocardium of both ventricles, according to delayed contrast-enhancement MRI. It confirms that the long-lasting adverse effects of various factors in CoAo which persist after the surgery, including a systolic overload of both ventricles, lead to myocardial hypertrophy, impairment of coronary vascular reserve, and even myocardial dystrophy [4].

Thus, the structural, functional, and biomechanical changes of the LV and aorta persist after the correction of CoAo. According to some data, LV functional values were restored faster than the geometrical measurements [23, 24]. It should be noted that in our study, the severity of fibrotic changes correlated with RVEF, rather than LVEF. This can be an indirect sign of severity, if there are no clinical manifestations of heart failure. The role of RV in the pathogenesis of myocardial fibrosis in patients with CoAo is generally an interesting and understudied issue. The delayed contrast enhancement MRI and the state-of-the-art tissue mapping MRI holds great promise in the search for diffuse and focal myocardial fibrosis.

In order to fully understand the pathological processes, the correlations we found between LV and RV structural and functional parameters and the blood flow values should be compared with the humoral markers of myocardial remodeling. Recent publications distinguish endothelin-1, ST2, galectin-3, norepinephrine, and NT-pro-BNP as biomarkers of abnormal LV changes in adults with CoAo. The biomarker levels enabled prediction of a persistent LV remodeling a year after the coarctation repair, although their ultimate predictive value is unknown [25].

After the restoration of the isthmus lumen, the remaining disturbances of the thoracic aortic viscoelasticity affect both the systolic and diastolic functions of the LV, as well as the filling of the heart. The left atrial volume both before and after a contraction, carotid artery wall thickness, and pulse wave velocity (PWV) in patients who had undergone surgery was significantly greater than in healthy patients [5].

The endothelial dysfunction more often affects the trunk vessels, with an increase in their intima/media thickness ratio. Cerebral vascular changes and hypertension cause cerebral symptoms. After the repair of CoAo, patients are still at the risk of aneurysmatic dilations of the aorta and cerebral vessels, and consequently, cerebrovascular accident and sudden death in the case of a rupture [4]. All our patients experienced changes in brachiocephalic vessels of various severity (asymmetry, hypoplasia, tortuosities). Vascular changes were combined with brain pathologies (focal lesion of the white matter, dilated perivascular spaces, retrocerebelular cysts, periventricular cyst) in 50% of children. Periventricular white matter is most predisposed to hypoxic and ischemic lesions. The pathogenesis of the white matter lesions is complex and is associated not only with impaired perfusion [26]. Disorders can develop within a short period of time both in the womb and at early neonatal age but are irreversible and persist after the surgery due to immaturity of the brain matters [26]. At a later stage, disorders are aggravated in the presence of hypertension. However, we found no data in the literature relating to the study of cerebral blood flow autoregulation in immature brains in children with CoAo and the monitoring of possible markers of the

ISSN 0022-9040. Kardiologiia. 2020;60(8). DOI: 10.18087/cardio.2020.8.n1094

brain pathological processes over time. We observed an unexpected inverse dependence of the brain changes on RVEF. This data may be indicative of an underestimated effect of the RV's condition in patients with CoAo. In such patients, the disturbed venous component of the brain blood flow (disturbed outflow) seems to be as important as the disturbed blood flow to the brain (increased inflow, increased BP). The complex changes in the blood supply of the brain with the involvement of the communicant vessels are likely to alter brain perfusion.

It remains unclear whether such changes are due to the underlying LV dysfunction or disturbed venous outflow and the RV, the effects of pathogenetic factors on the immature brain at early age, as noted above, or whether the mechanism is more complex. The RV is of paramount importance in the life of a fetus, since it delivers about 55% of total cardiac output [27]. The isthmus is akin to a hemodynamic bridge in a fetus' body between the RV and LV outputs. The altered intracardiac circulation and fetal blood flow affect the distal vascular system of the fetus. At birth, LV activity gradually increases as oxygen is delivered to the tissues. However, a reserve limited in pressure or volume overload should be considered. Perhaps, in CoAo and especially in combination with hypoplasia, the RV condition, under a certain combination of factors, will be initially essential to the severity of changes in the brain. Further research is still required to find an ultimate answer. The new pathogenetic patterns of blood flow (changes in the velocity and volume of blood flow in combination with an altered blood flow profile, the appearance of additional abnormal flows in the aorta and brachiocephalic vessels throughout the heart cycle) or brain damage risk factors might be identified.

Thus, 4D Flow helps to for a better understanding of the pathophysiology of blood circulation in patients with CoAo. It also helps determine the role and the impact of hemodynamics on the heart and vessels, and assess the recovery of the normal physiological profile of blood flow after surgical procedures. We did not perform a comparative analysis of patients CoAo and healthy individuals. This study is a pilot study of the clinical use of the 4D Flow MRI protocol in patients with CoAo. We plan to carry out a more in-depth study of blood flow in a large statistical sample.

Conclusion

The 4D-processing of MR images of any vascular system enables a detailed study of blood flow in natural conditions to be carried out. It also provides potential advantages in the complete examination of patients with coarctation of the aorta during the case follow-up. Larger studies and long-term follow-up of patients with identified blood flow pathologies are needed to define the relationship between altered blood flow in the thoracic aorta and markers of post-repair pathology (changes in the velocity and volume of blood flow combined with abnormal blood flow geometry in the aorta and its branches within the cardiac cycle).

No conflict of interest is reported.

The article was received on 20/03/2020

REFERENCES

1. Nozaki Y, Nakayama-Inaba K, Ishizu T, Iida N, Kato Y, Hiramatsu Y et al. Endothelial Dysfunction of Conduit Arteries in Patients with Repaired Coarctation of the Aorta. International Heart Journal. 2018;59(6):1340–5. DOI: 10.1536/ihj.17-564
2. Hope MD, Meadows AK, Hope TA, Ordovas KG, Saloner D, Reddy GP et al. Clinical evaluation of aortic coarctation with 4D flow MR imaging. Journal of Magnetic Resonance Imaging. 2010;31(3):711–8. DOI: 10.1002/jmri.22083
3. Dijkema EJ, Leiner T, Grotenhuis HB. Diagnosis, imaging and clinical management of aortic coarctation. Heart. 2017;103(15):1148–55. DOI: 10.1136/heartjnl-2017-311173
4. Kim A.I., Rogova T.V., Vereshchagina A.M., Mashina T.V. Coarctation of the aorta: does the patient, operated at an early age, have to be observed later? Creative cardiology. 2015;1:46–55. [Russian: Ким А.И., Рогова Т.В., Верещагина А.М., Машина Т.В. Коарктация аорты: нуждается ли пациент, оперированный в раннем возрасте, в дальнейшем наблюдении? Креативная кардиология. 2015;1:46-55]
5. Voges I, Kees J, Jerosch-Herold M, Gottschalk H, Trentmann J, Hart C et al. Aortic stiffening and its impact on left atrial volumes and function in patients after successful coarctation repair: a multiparametric cardiovascular magnetic resonance study. Journal of Cardiovascular Magnetic Resonance. 2016;18(1):56. DOI: 10.1186/s12968-016-0278-6
6. Pineda J, Abad P, Mesa S, Rascovsky S, Delgado J. Clinical Applications of the 4D Flow Technique in the Hemodynamic Evaluation of Congenital Heart Diseases. Revista Colomb. Radioljgy. 2018;29(2):4901–7. [Av. at: https://www.webcir.org/revistavirtual//articulos/2018/3_agosto/col/aplicacion_eng.pdf]
7. Stankovic Z, Allen BD, Garcia J, Jarvis KB, Markl M. 4D flow imaging with MRI. Cardiovascular Diagnosis and Therapy. 2014;4(2):173–92. DOI: 10.3978/j.issn.2223-3652.2014.01.02
8. Ota H, Higuchi S, Sun W, Ueda T, Takase K, Tamura H. Four-Dimensional Flow Magnetic Resonance Imaging for Cardiovascular Imaging: from Basic Concept to Clinical Application. Cardiovascular Imaging Asia. 2018;2(2):85–96. DOI: 10.22468/cvia.2018.00045
9. Ralovich K, Itu L, Vitanovski D, Sharma P, Ionasec R, Mihalef V et al. Noninvasive hemodynamic assessment, treatment outcome prediction and follow-up of aortic coarctation from MR imaging: Noninvasive assessment of coarctation from MRI. Medical Physics. 2015;42(5):2143–56. DOI: 10.1118/1.4914856
10. Rengier F, Delles M, Eichhorn J, Azad Y-J, von Tengg-Kobligk H, Ley-Zaporozhan J et al. Noninvasive pressure difference mapping derived from 4D flow MRI in patients with unrepaired and repaired aortic coarctation. Cardiovascular Diagnosis and Therapy. 2014;4(2):97–103. DOI: 10.3978/j.issn.2223-3652.2014.03.03
11. Ou P, Mousseaux E, Celermajer DS, Pedroni E, Vouhe P, Sidi D et al. Aortic arch shape deformation after coarctation surgery: Effect on blood pressure response. The Journal of Thoracic and Cardiovascular Surgery. 2006;132(5):1105–11. DOI: 10.1016/j.jtcvs.2006.05.061
12. Markl M, Kilner PJ, Ebbers T. Comprehensive 4D velocity mapping of the heart and great vessels by cardiovascular magnetic resonance.

Journal of Cardiovascular Magnetic Resonance. 2011;13(1):7. DOI: 10.1186/1532-429X-13-7
13. Frydrychowicz A, Berger A, Munoz del Rio A, Russe MF, Bock J, Harloff A et al. Interdependencies of aortic arch secondary flow patterns, geometry, and age analysed by 4-dimensional phase contrast magnetic resonance imaging at 3 Tesla. European Radiology. 2012;22(5):1122–30. DOI: 10.1007/s00330-011-2353-6
14. Ou P, Celermajer DS, Raisky O, Jolivet O, Buyens F, Herment A et al. Angular (Gothic) aortic arch leads to enhanced systolic wave reflection, central aortic stiffness, and increased left ventricular mass late after aortic coarctation repair: Evaluation with magnetic resonance flow mapping. The Journal of Thoracic and Cardiovascular Surgery. 2008;135(1):62–8. DOI: 10.1016/j.jtcvs.2007.03.059
15. Sophocleous F, Biffi B, Milano EG, Bruse J, Caputo M, Rajakaruna C et al. Aortic morphological variability in patients with bicuspid aortic valve and aortic coarctation. European Journal of Cardio-Thoracic Surgery. 2019;55(4):704–13. DOI: 10.1093/ejcts/ezy339
16. Quail MA, Segers P, Steeden JA, Muthurangu V. The aorta after coarctation repair – effects of calibre and curvature on arterial haemodynamics. Journal of Cardiovascular Magnetic Resonance. 2019;21(1):22. DOI: 10.1186/s12968-019-0534-7
17. Canniffe C, Ou P, Walsh K, Bonnet D, Celermajer D. Hypertension after repair of aortic coarctation – A systematic review. International Journal of Cardiology. 2013;167(6):2456–61. DOI: 10.1016/j.ijcard.2012.09.084
18. Bhatt AB, Defaria Yeh D. Long-term outcomes in coarctation of the aorta: an evolving story of success and new challenges. Heart. 2015;101(15):1173–5. DOI: 10.1136/heartjnl-2015-307641
19. Coogan JS, Humphrey JD, Figueroa CA. Computational simulations of hemodynamic changes within thoracic, coronary, and cerebral arteries following early wall remodeling in response to distal aortic coarctation. Biomechanics and Modeling in Mechanobiology. 2013;12(1):79–93. DOI: 10.1007/s10237-012-0383-x
20. Sinelnikov Yu.S., Gasanov E.N., Orehova E.N. Vascular dysfunction in patients with coarctation of the aorta: two-year results after early correction. Circulation Pathology and Cardiac Surgery. 2017;21(1):62–8. [Russian: Синельников Ю.С., Гасанов Э.Н., Орехова Е.Н. Сосудистая дисфункция у пациентов с коарктацией аорты: двухлетние результаты после коррекции в раннем возрасте. Патология кровообращения и кардиохирургия. 2017;21(1):62-8]. DOI: 10.21688/1681-3472-2017-1-62-68
21. Sinelnikov Yu.S., Kshanovskaya M.S., Prokhorova D.S., Nartsissova G.P., Gorbatykh A.V., Ivantsov S.M. et al. Surgical correction of Aortic Coarctation: does it always satisfy expectations? Siberian Medical Journal (Tomsk). 2013;28(4):55–8. [Russian: Синельников Ю.С., Кшановская М.С., Прохорова Д.С., Нарциссова Г.П., Горбатых А.В., Иванцов С.М. и др. Хирургическая коррекция коарктации аорты, всегда ли оправданы ожидания? Сибирский медицинский журнал (г. Томск). 2013;28(4):55-8]
22. Ntsinjana HN, Biglino G, Capelli C, Tann O, Giardini A, Derrick G et al. Aortic arch shape is not associated with hypertensive response to exercise in patients with repaired congenital heart diseases. Journal of Cardiovascular Magnetic Resonance. 2013;15(1):101. DOI: 10.1186/1532-429X-15-101
23. Prokhorova D.S., Nartsissova G.P., Gorbatykh Yu.N., Sinel'nikov Yu.S., Gorbatykh A.V. Dynamics of left ventricular adaptation processes in young patients with aortic coarctation before and after surgical correction. Circulation Pathology and Cardiac Surgery. 2012;16(1):11–5. [Russian: Прохорова Д.С., Нарциссова Г.П., Горбатых Ю.Н., Синельников Ю.С., Горбатых А.В. Динамика процессов адаптации левого желудочка у больных раннего возраста с коарктацией аорты до и после хирургической коррекции. Патология кровообращения и кардиохирургия. 2012;16(1):11-5]
24. Sinelnikov Yu.S., Orekhova E.N., Matanovskaya T.V. Left ventricular mechanical function and aortic elastic properties in newborns with aortic coarctation. Prognostic significance of obtained data. Circulation Pathology and Cardiac Surgery. 2018;22(3):10–6. [Russian: Синельников Ю.С., Орехова Е.Н., Матановская Т.В. Механическая функция левого желудочка и эластические свойства аорты у новорожденных с коарктацией аорты. Ценность получаемых данных для прогноза. Патология кровообращения и кардиохирургия. 2018;22(3):10-6]. DOI: 10.21688/1681-3472-2018-3-10-16
25. Frank BS, Urban TT, Lewis K, Tong S, Cassidy C, Mitchell MB et al. Circulating biomarkers of left ventricular hypertrophy in pediatric coarctation of the aorta. Congenital Heart Disease. 2019;14(3):446–53. DOI: 10.1111/chd.12744
26. Klayman Ch, Sery I. Hemodynamics and cardiology. Problems and contradictions in neonatology. -M.: Logosfera;2015. – 512 p. [Russian: Клайнман Ч., Сери И. Гемодинамика и кардиология. Проблемы и противоречия в неонатологии. пер с англ. – М.: Логосфера; 2015. –512с]. ISBN 978-5-98657-038-9
27. Hoffman D. Children's cardiology. – M.: Praktika;2006. – 543 p. [Russian: Хоффман Дж.(ред.) Детская кардиология. пер с англ. – М.: Практика; 2006. – 543с]. ISBN 5-89816-071-X

ISSN 0022-9040. Kardiologiia. 2020;60(8). DOI: 10.18087/cardio.2020.8.n1094